

IDENTIFICATION OF TWO CLASSES OF GAMMA-RAY BURSTS

CHRYSSA KOUVELIOTOU¹

Universities Space Research Association

CHARLES A. MEEGAN, GERALD J. FISHMAN, AND NARAYANA P. BHAT²

NASA/Marshall Space Flight Center, Huntsville, AL 35812

AND

MICHAEL S. BRIGGS, THOMAS M. KOSHUT, WILLIAM S. PACIESAS, AND GEOFFREY N. PENDLETON

Department of Physics, University of Alabama in Huntsville, Huntsville, AL 35899

Received 1993 April 5; accepted 1993 May 28

ABSTRACT

We have studied the duration distribution of the gamma-ray bursts of the first BATSE catalog. We find a bimodality in the distribution, which separates GRBs into two classes: short events (<2 s) and longer ones (>2 s). Both sets are distributed isotropically and inhomogeneously in the sky. We find that their durations are anticorrelated with their spectral hardness ratios: short GRBs are predominantly harder, and longer ones tend to be softer. Our results provide a first GRB classification scheme based on a combination of the GRB temporal and spectral properties.

Subject heading: gamma rays: bursts

1. INTRODUCTION

Gamma-ray burst (GRB) studies over the last 20 years have not succeeded in revealing telltale properties that would help identify the nature of their emission sites. Moreover, there exist no concrete counterpart identifications in any other wavelength within the well-defined GRB error boxes (Hurley 1991 and references therein) that would point toward a known parent population for the phenomenon. Recent results (Meegan et al. 1991) from the Burst and Transient Source Experiment (BATSE) (Fishman et al. 1989) on the *Compton Gamma-Ray Observatory* (CGRO) have shown that the sky distribution of the GRB sources is isotropic, but not homogeneous. Any attempt to identify GRB subclasses based on similarities in their spatial, spectral, or morphological properties has failed so far (Briggs et al. 1993; Fishman et al. 1993). We present here a study of one of the GRB global properties, namely their duration distribution, which has led to the confirmation of their division into two subclasses. This duration bimodality is linked for the first time with a different average spectral hardness associated with each class.

2. DURATION DISTRIBUTION

The distribution of GRB durations has been studied extensively in the past (Cline & Desai 1974; Mazets et al. 1981; Norris et al. 1984; Klebesadel 1990; Hurley 1991). Most studies agree that there is a hint of bimodality with the separation being in the 0.5–4 s range. There are several reasons that the previous data sets could not establish the bimodal nature of the distribution: lack of instrument trigger sensitivity to short events, low temporal resolution, difficulty of confirmation of a very short event as a burst in an often noisy data set, etc. They have all led to biases against detection of short events. The first BATSE catalog (Fishman et al. 1993) presents

a complete, confirmed set of 260 GRBs, detected with unprecedented sensitivity over the instrument's first year of operation (1991 April 21 to 1992 March 5).

2.1. The T_{90} and T_{50} Algorithm

The criteria for determining a GRB duration have (widely) varied over the past, without an accepted consensus for a "duration algorithm." We introduced in the first BATSE catalog (Fishman et al. 1993) an unbiased and reproducible way of estimating durations. We have used the sum of the counts >25 keV in the triggered detectors. Using summed detector data reduces the effect of Earth scattering and the dependence of the detector response on the burst arrival direction. We define T_{90} as the time during which the cumulative counts increase from 5% to 95% above background, thus encompassing 90% of the total GRB counts. T_{50} is defined similarly to include 50% of the counts. The times thus defined are an intensity-independent measure of duration, unlike previous definitions.

In most cases the data available afforded very accurate measurements for both times. This procedure failed whenever there existed data gaps during a burst readout. Thus, of the 260 GRBs contained in the first BATSE catalog, we have T_{90} and T_{50} values for 222. In some extreme cases the burst was coincident with a high local background, and in a few cases the high time resolution data needed for the very short events were missing due to telemetry gaps; the uncertainties in these T_{90} and T_{50} calculations are reflected in their large errors δT_{90} and δT_{50} . Finally, in some of the bursts, we have not included possible precursor activity when it was relatively weak and could not be confirmed as associated with the burst by having a well-determined, coincident location.

2.2. The T_{90} and T_{50} Distributions

The solid line in Figure 1a shows the uncorrected distribution of the 222 values for T_{90} . To account for the time errors δT_{90} in each histogram bin, we have assumed that each T_{90} is represented by a Gaussian of standard deviation given by δT_{90} .

¹ Present address: NASA/Marshall Space Flight Center, Huntsville, AL 35812.

² NRC/NASA Senior Research Associate; on leave from Tata Institute of Fundamental Research, Bombay 400 005, India.

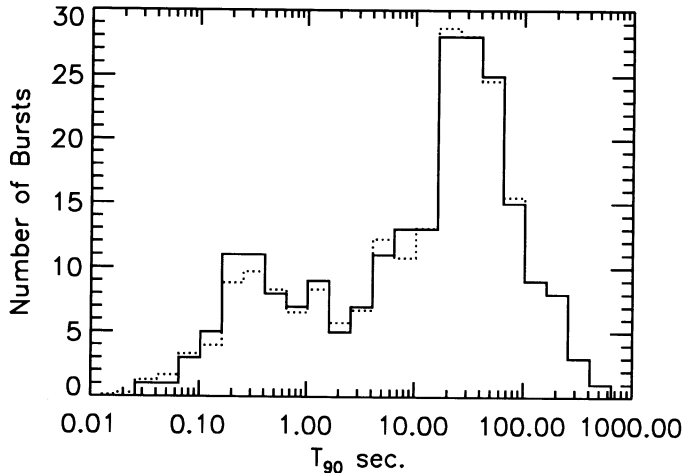


FIG. 1a

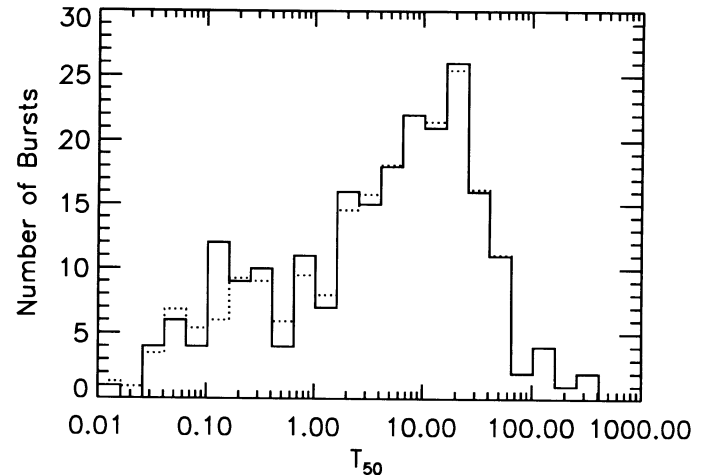


FIG. 1b

FIG. 1.—(a) Distribution of T_{90} for the 222 GRBs of the first BATSE catalog. (b) Distribution of T_{50} for the same GRB set. Solid lines are the histograms of the raw data; dotted lines are the error-convolved histograms as explained in the text.

Each error-convolved histogram bin is then derived by adding the overlapping areas of all Gaussians that fall within its boundaries. The convolved distribution is plotted with a dotted line on Figure 1a; we notice that the inclusion of the errors has expanded the short duration range (where the uncertainties are larger) but has not affected the longer duration bursts.

Both distributions of Figure 1 show a dip around 2 s. The dip is not an instrumental artifact: BATSE's trigger sensitivity is maximum near 1 s, which is its longest trigger time scale. Although it is difficult to quantitatively assess the statistical significance of the dip, we estimate the convex, unimodal distributions are rejected at the $2\text{--}3\sigma$ level. We have fitted a quadratic function between the two peaks in the histogram and determined its minimum to be at $T_{90} = 1.2 \text{ s} \pm 0.4 \text{ s}$, which rounded off to the next integer bin edge, is 2.0 s. This effectively divides the 222 GRBs into two subsets: one containing 58 short events ($T_{90} < 2.0 \text{ s}$) with a logarithmic mean T_{90} of $0.33 \text{ s} \pm 0.21 \text{ s}$ and a second of 164 longer GRBs with a mean of $26.2 \text{ s} \pm 1.7 \text{ s}$.

The fraction of short events in the data bases derived with various experiments does not seem to vary significantly:

SIGNE (on *Venera 11/12*) reports 25% (Diyachkov et al. 1980); the *International Sun Earth Explorer 3 (ISEE 3)* shows 29% (Norris et al. 1984), albeit with a limited sample; the Phebus instrument on *Granat* has 27% (Dezalay et al. 1991); and for BATSE the same fraction amounts to 26% of the first catalog data. The KONUS experiments on *Venera 11/12* and *13/14*, however, show significantly smaller percentages, 7% and 16%, respectively. One explanation of this discrepancy could be the detection threshold for the KONUS experiments, which increased with decreasing GRB duration (Mazets et al. 1981).

Comparison of the duration distributions obtained by previous observers (see Hurley 1991) with the T_{90} distribution shows that the BATSE data have a factor of 2 higher average durations. The arithmetic mean of the T_{90} values is $37.6 \text{ s} \pm 2.7 \text{ s}$ versus the mean of 18.3 s for 616 GRBs compiled by Hurley (1991). One possible explanation of this shift in mean duration could be a systematic effect of instrumental sensitivity. BATSE, with its unprecedented sensitivity, would see what previous experiments would have called an average GRB for a much longer time. If that is indeed the case, raising the instrument sensitivity would bring the average duration to a lower value.

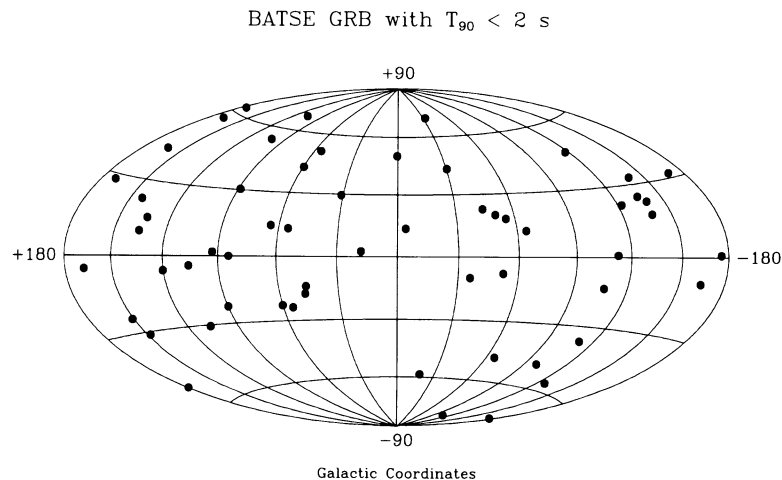


FIG. 2.—The sky map distribution of the 58 short ($< 2 \text{ s}$) GRBs

TABLE 1
STATISTICS FOR THE 58 BURSTS WITH $T_{90} < 2$ s

Statistic ^a	Moment	Coordinate System	Value Expected for Isotropy with Uniform Sky Exposure	Value Expected for Isotropy with BATSE Sky Exposure	Observed Value (with propagation of location errors)
$\langle \cos \theta \rangle$	Dipole	Galactic	0 ± 0.076	-0.013 ± 0.076	-0.073 ± 0.014
$\langle \sin^2 b - \frac{1}{3} \rangle$	Quadrupole	Galactic	0 ± 0.039	-0.005 ± 0.039	-0.048 ± 0.011
\mathcal{H}	Dipole	Independent	3.0 ± 2.4	3.1 ± 2.4	2.8 ± 0.6
\mathcal{B}	Quadrupole	Independent	5.0 ± 3.2	5.4 ± 3.2	2.2 ± 0.9
$\langle \sin \delta \rangle$	Dipole	Equatorial	0 ± 0.076	0.026 ± 0.076	0.119 ± 0.014
$\langle \sin^2 \delta - \frac{1}{3} \rangle$	Quadrupole	Equatorial	0 ± 0.039	0.026 ± 0.039	0.017 ± 0.013

^a θ is the angle between a burst and the Galactic center, b is galactic latitude, and δ is declination.

The T_{50} distribution for the same 222 GRBs (Fig. 1b) effectively does this. We notice that the average value of T_{50} is $16.3 \text{ s} \pm 1.0 \text{ s}$, similar to KONUS and half of that for BATSE's T_{90} 's. Hence what we see is a convincing effect of different detection thresholds on the GRB durations, which strengthens the case of using a single experiment to derive statistics on GRB duration distributions. We also notice that the duration bimodality is not as significant in the T_{50} distribution; this again is consistent with a "tip of the iceberg" effect.

We have searched for clusterings in the burst arrival times for short and long events: both samples are entirely consistent with Poisson distributions. The arrival rates are 0.2 and 0.8 per day for the short and long GRBs, respectively.

In the following we will consider the set of the 58 short GRBs with $T_{90} < 2$ s as a different class and study their global properties.

3. SPATIAL DISTRIBUTIONS: ISOTROPY AND HOMOGENEITY TESTS

Figure 2 shows the sky distribution of the short events; although the sample is limited, we can still see that their distribution is isotropic. Table 1 contains the values of their various dipole and quadrupole statistics (Briggs 1993). In most cases the observed values differ by about 1 standard deviation or less from the values expected for isotropy. We have also examined the distribution of the angular separations of GRB pairs and found no evidence for clustering.

Similarly, the statistics of the longer events are consistent with an isotropic distribution as expected from the overall isotropy of the 260 GRBs from the first BATSE catalog (Fishman et al. 1993).

Whenever we have data gaps during a burst accumulation, we do not compute the V/V_{\max} for the event, as is explained in Fishman et al. (1993). We have both T_{90} and V/V_{\max} values on the 64 ms trigger time scale for 48 short events and 100 long ones. The $\langle V/V_{\max} \rangle$ values are 0.302 ± 0.038 and 0.367 ± 0.030 , respectively. There is no significant difference between the two means: they are consistent with each other and both are inconsistent with homogeneity. The same trend is evident from Figure 3, which shows the log N -log P diagram for the short (58) and long (164) GRB sets, together with a homogeneous distribution (dashed line). We conclude that both sets are isotropic and inhomogeneous, in agreement with the overall BATSE GRB results.

4. HARDNESS RATIOS VERSUS T_{90}

We have integrated the counts above background during T_{90} for the 222 GRBs in four discriminator channels with

energy ranges of 25–50, 50–100, 100–300, and > 300 keV. We define as $HR_{3/21}$ the ratio of total counts in the 100–300 keV and 25–100 keV energy ranges, and as HR_{32} the ratio of total counts in the 100–300 keV and 50–100 keV energy range. Figure 4 (right panel) shows the scatter plot of the hardness ratios HR_{32} versus T_{90} . The Spearman rank-order correlation coefficient (Press et al. 1992) between HR_{32} and T_{90} is -0.375 ; the probability of a fluctuation causing a chance correlation at this level is $\sim 10^{-8}$. The density distributions of the hardness ratios are shown as two histograms in the left panel of Figure 4. Short events are predominantly harder, while longer events are predominantly softer, as expected from the high correlation between hardness ratios and durations. The same trend is seen with the $HR_{3/21}$ distribution.

Table 2 contains values for both HR distributions for the means and weighted means calculated separately for the two GRB classes previously identified. The average values for the short events are clearly higher than the ones for the longer events. This result has also been seen in the Phebus data (Dezalay et al. 1991), albeit between higher energy ranges (0.3–7 MeV to 100–300 keV). Dezalay et al., however, were unable to detect a duration bimodality in their small sample of 66 GRBs. We believe that our data confirm these earlier

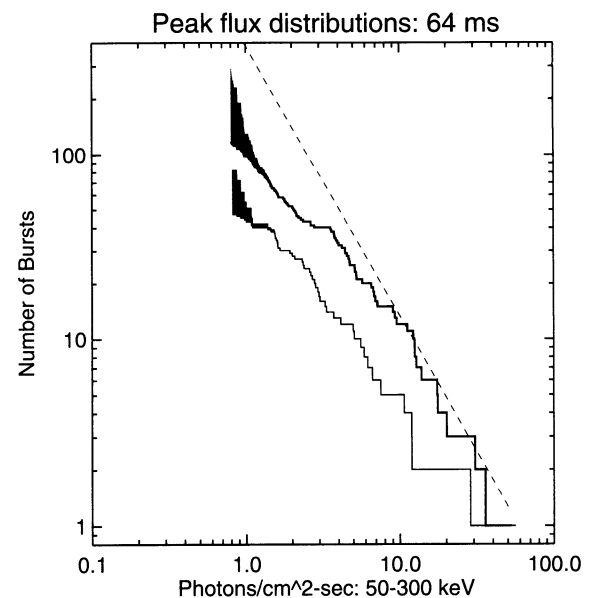


FIG. 3.—Log N -log P distributions for the long (upper curve) and for the short (lower curve) GRBs. The peaks are integrated with 64 ms over 50–300 keV. The shaded regions represent the range of Earth scattering corrections.

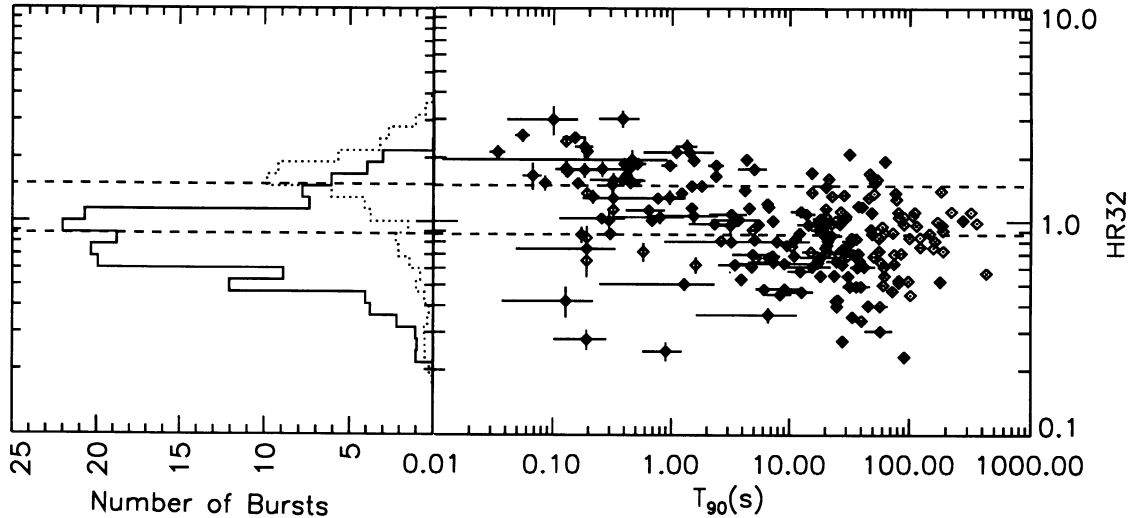


FIG. 4.—*Left*: Separate hardness ratio histograms for the two duration classes. The solid line shows events with $T_{90} > 2$ s, and the dotted line depicts < 2 s long events. *Right*: Hardness ratios HR_{32} vs. T_{90} scatter plot. The dashed lines on both plots correspond to the mean hardness ratio of the two duration classes.

TABLE 2

STATISTICS OF THE HARDNESS RATIOS FOR THE TWO GRB CLASSES

Class	Mean	Weighted Mean
$HR_{3/21}$		
< 2 s	0.99 ± 0.06	0.499 ± 0.004
> 2 s	0.49 ± 0.02	0.449 ± 0.0003
HR_{32}		
< 2 s	1.49 ± 0.08	1.065 ± 0.008
> 2 s	0.87 ± 0.03	0.8456 ± 0.00006

5. DISCUSSION

We have linked here for the first time the duration bimodality with the hardness-duration correlation of GRBs. Previous studies have reported evidence for either the former (Cline & Desai 1974; Mazets et al. 1981; Klebesadel 1990; Norris et al. 1984; Hurley 1991) or the latter (Dezalay et al. 1991). Our study shows that the two classes separated by duration are also associated with significantly different average hardness ratios. We find that the short events have the same peak intensity range as the longer ones; this makes the total amount of energy released by the two types significantly different. Both short and long GRBs have isotropic but inhomogeneous spatial distributions. All evidence suggests that both GRB subsets originate from the same type of objects. Different geometries of their emission sites (with respect to the observer) may be responsible for the spectral and temporal differences between the classes.

We wish to express our thanks to Bohdan Paczyński, Jan van Paradijs, and Gerry Share for fruitful discussions and to J. Ostriker for suggesting to us the T_{50} algorithm as a measure for the GRB durations.

results and provide the first evidence of the continuity of the hardness-duration correlation over the whole GRB observable spectrum.

The peak intensities (integrated over 256 ms and between 25–300 keV) versus T_{90} do not show a significant trend. Similarly, we find no trend in the peak hardness ratio versus peak intensity diagram as already reported (for different integration intervals) by Kouveliotou et al. (1992). A more detailed study of peak intensities versus spectral hardness is given by Paciasas et al. (1991) and by Pendleton et al. (1993).

REFERENCES

- Briggs, M. S. 1993, *ApJ*, 407, 126
 Briggs, M. S., et al. 1993, in preparation
 Cline, T. L., & Desai, U. D. 1974, in *Proc. 9th ESLAB Symp.* (Noordwijk: ESRO), 37
 Dezalay, J.-P., et al. 1991, in *Gamma-Ray Bursts Huntsville, AL 1991*, ed. W. S. Paciasas & G. J. Fishman (AIP Conf. Proc. 265) (New York: AIP), 304
 Diyackov, A. V., et al. 1980, *Adv. Space Res.*, 3, 211
 Fishman, G. J., et al. 1989, in *Proc. of the GRO Science Workshop*, ed. W. N. Johnson (NASA/GSFC), 39
 Fishman, G. J., et al. 1993, in preparation
 Hurley, K. 1991, in *Gamma-Ray Bursts Huntsville, AL 1991*, ed. W. S. Paciasas & G. J. Fishman (AIP Conf. Proc. 265) (New York: AIP), 3
 Klebesadel, R. W. 1990, in *Gamma Ray Bursts*, ed. C. Ho, R. I. Epstein, & E. E. Fenimore (Cambridge: Cambridge Univ. Press), 161
 Kouveliotou, C., et al. 1992, in *Proc. CGRO Symposium in St. Louis*, ed. N. Geherels & M. Friedlauder, in press
 Mazets, E. P., et al. 1981, *Ap&SS*, 80, 3
 Meegan, C. A., et al. 1991, *Nature*, 355, 143
 Norris, J. P., et al. 1984, *Nature*, 308, 434
 Paciasas, W. S., et al. 1991, in *Gamma-Ray Bursts Huntsville, AL 1991*, ed. W. S. Paciasas & G. J. Fishman (AIP Conf. Proc. 265) (New York: AIP), 190
 Pendleton, G. N., et al. 1993, in preparation
 Press, W. H., et al. 1992, *Numerical Recipes* (2d ed.; Cambridge: Cambridge Univ. Press)